UDC 340.5

OCEAN BATHYMETRY RECONSTRUCTION USING RADIATIVE TRANSFER THEORY

Andrei Sushchenko[1,2] *and Elizaveta Liu*[1]

[1] Far Eastern Federal University, Vladivostok, Russia

[2]Institute of Applied Mathematics FEB RAS, Vladivostok, Russia

e-mail: sushchenko.aa@dvfu.ru, liu.er@students.dvfu.ru.

Abstract: Based on the mathematical model of the propagation of an acoustic signal in a fluctuating medium, the inverse problem is formulated for determination a function that describes the deviation of the seabottom level from the average specified horizontal plane. In the double scattering approximation and the narrow directivity pattern of the receiving antenna, the solution of the direct problem is obtained. As a solution of the inverse problem, a nonlinear differential equation is obtained for the function describing the deviation of the seabottom relief. A numerical analysis of the solution is carried out and the influence of a double-scattered signal on the retrieval of the bathymetric function is investigated.

Key words: Radiative transfer equation, scattering, bathymetry, remote sensing, sonar.

The study of the ocean is still a priority for the world community. A lot of research complexes are being developed to solve bathymetry problems (see e.g. [1-4]). Nowadays, the problem of mapping the ocean bottom using side scan sonars (SSS) which were equipped of an autonomous unmanned underwater vehicle, is very relevant and promising. The study of the ocean properties by using SSS generates a very interesting problem of determining the relief of the sea bottom. The sonar operation is based on the periodic emission of pulsed sound parcels and the detection of reflected echo signal from remote seabed domains. When the sonar antenna is moved, an acoustic image is formed on the starboard and portside of the underwater vehicle.

The process of propagation of acoustic radiation is described by the radiative transfer equation [4, 5]:

$$\frac{1}{c}\frac{\partial I}{\partial t} + \boldsymbol{k}\cdot\nabla_r I(\boldsymbol{r},\boldsymbol{k},t) + \mu\, I(\boldsymbol{r},\boldsymbol{k},t) = \frac{\sigma}{2\pi}\int\limits_{\Omega} I(\boldsymbol{r},\boldsymbol{k}',t)d\boldsymbol{k}' + J(\boldsymbol{r},\boldsymbol{k},t), \qquad (1)$$

where $\in \mathbb{R}^2$, $t \in [0,\mathrm{T}]$ and wave vector $\boldsymbol{k}$ belongs to the unique sphere $\Omega = \{\mathrm{k} \in \mathrm{R}^2 : |\mathrm{k}| = 1\}$. The function $I(\boldsymbol{r},\boldsymbol{k},t)$ is interpreted as radiation intensity in moment t in point $\boldsymbol{r}$, propagated in the direction $\boldsymbol{k}$ with constant velocity c. μ and σ denote the attenuation and the scattering coefficients, correspondingly. $J(\boldsymbol{r},\boldsymbol{k},t)$ describes the density of inner sources.

The process of echo signal propagation occurs in the domain $G := \{\boldsymbol{r} \in \mathbb{R}^2 : r_2 > -l + u(r_1)\}$, which is the upper half-space bounded from below by the curve, $\partial G = \gamma = \{\boldsymbol{y} \in \mathbb{R}^2 : y_2 = -l + u(y_1)\}$, where the function $u(y_1)$ describes the change of the ocean bottom relief.

We assume that the function $J(\boldsymbol{r},\boldsymbol{k},t)$ describes a point isotropic sound source [6]:

$$J(\boldsymbol{r},\boldsymbol{k},t) = J_0\, \delta(\boldsymbol{r})\, \delta(t), \qquad (2)$$

where δ denotes the Dirac delta function and J_0 is the source power.

Initial and boundary conditions for (1):

$$I|_{t<0} = 0, \qquad (3)$$

$$I(\boldsymbol{y},\boldsymbol{k},t) = 2\,\sigma_d \int_{\Omega_+(\boldsymbol{y})} |\boldsymbol{n}(\boldsymbol{y})\cdot\boldsymbol{k}'|\, I(\boldsymbol{y},\boldsymbol{k}',t)d\boldsymbol{k}',\ \ \boldsymbol{y}\in\gamma, \boldsymbol{k}\in\Omega_-(\boldsymbol{y}), \qquad (4)$$

where $\Omega_\pm(\boldsymbol{y}) = \{\boldsymbol{k}\in\Omega, \mathrm{sgn}(\boldsymbol{k}\cdot\boldsymbol{n}(\boldsymbol{y})) = \pm 1\}$, σ_d denotes the constant seabottom reflection coefficient, $\boldsymbol{n}(\boldsymbol{y})$ denotes the exterior normal to ∂G.

We introduce an additional condition on the carrier of the receiving antenna, which is concentrated at the point $\boldsymbol{O} = (0,0)$:

$$\int_{\Omega_+(\boldsymbol{y})} S^{\pm}(\boldsymbol{k}) I|_{\Gamma^{\pm}}(\boldsymbol{O},\boldsymbol{k},t)d\boldsymbol{k} = I^{\pm}(t).$$

Here, the function $S^{\pm}(\boldsymbol{k})$, when $\boldsymbol{k} \in \{\boldsymbol{k} \in \Omega : \operatorname{sgn}(k_1) = \pm 1\}$, are characterizes the receiving antenna pattern on the starboard and the portside of the carrier, respectively; $I^{\pm}(t)$ determines the measured total intensity on starboard and portside along the direction of movement of the antenna carrier; $I|_{\Gamma^{\pm}}(\boldsymbol{r},\boldsymbol{k},t) = \lim_{\epsilon\to 0} I(\boldsymbol{r} \pm \epsilon\boldsymbol{k},\boldsymbol{k},t \pm \epsilon)$.

The solution of the initial-boundary problem (1), (3), (4) is deduced to the integral equation [5, 9]:

$$I(\boldsymbol{r},\boldsymbol{k},t) = \int_0^{d(\boldsymbol{r},-\boldsymbol{k})} exp(-\mu t') J_0\left(\boldsymbol{r} - t'\boldsymbol{k},\boldsymbol{k},t - \frac{t'}{c}\right) dt +$$
$$+ 2\sigma_d \exp\big(-\mu d(\boldsymbol{r},-\boldsymbol{k})\big) \int_{\Omega_+(\boldsymbol{r}-d(\boldsymbol{r},-\boldsymbol{k})\boldsymbol{k})} |n\cdot \boldsymbol{k}'|\ I_{\Gamma^+}\left(\boldsymbol{r} - d(\boldsymbol{r},-\boldsymbol{k})\boldsymbol{k},\boldsymbol{k}',t - \frac{d(\boldsymbol{r},-\boldsymbol{k})}{c}\right) d\boldsymbol{k}' \tag{5}$$
$$+$$
$$+ \int_0^{d(\boldsymbol{r},-\boldsymbol{k})} \exp(-\mu t') \frac{\sigma}{4\pi}\int_{\Omega} I\left(\boldsymbol{r} - t'\boldsymbol{k},\boldsymbol{k},t - \frac{t'}{c}\right) d\boldsymbol{k}' dt'.$$

Here, $d(\boldsymbol{r},-\boldsymbol{k})$ denotes the distance from the point $\boldsymbol{r} \in G$ in the direction $-\boldsymbol{k}$ to the boundary of the region G.

For solving (5) authors construct an iteration method. Denote the initial approximation as

$$I_0 = \int_0^{d(\boldsymbol{r},-\boldsymbol{k})} \exp(-\mu t') J_0\left(\boldsymbol{r} - t'\boldsymbol{k},\boldsymbol{k},t - \frac{t'}{c}\right) dt'.$$

Thus, the solution of the direct problem in the double scattering approximation and in the assumption that G is non-scattering ($\sigma = 0$), can be represented in the following form:

$$I^{\pm}(t) = X_{[0,\pm\infty]} \frac{8\,\sigma_d\, J_0 \exp(-\mu c t)\ \left(y_1\, u'_{y_1} + l - u(y_1)\right)^2}{c^2 t^3\ \left|u'_{y_1}(l - u(y_1)) - y_1\right| \sqrt{1 + \left(u'_{y_1}\right)^2}} +$$
$$+ 4\sigma_d^2 J_0 \int_{-\infty}^{+\infty}\int_{-\infty}^{+\infty} S^{\pm}(\boldsymbol{k}) \frac{\exp(-\mu|\boldsymbol{y}|)}{|\boldsymbol{y}|} \exp(-\mu|\boldsymbol{y}-\boldsymbol{z}|) \frac{\exp(-\mu|\boldsymbol{z}|)}{|\boldsymbol{z}|} \left|\boldsymbol{n}(\boldsymbol{y}) \cdot \frac{\boldsymbol{y}}{|\boldsymbol{y}|}\right| \times \tag{6}$$
$$\times \left|\boldsymbol{n}(\boldsymbol{y}) \cdot \frac{\boldsymbol{z}}{|\boldsymbol{z}|}\right| \delta\left(t - \frac{|\boldsymbol{y}-\boldsymbol{z}|}{c} - \frac{|\boldsymbol{z}|}{c} - \frac{|\boldsymbol{y}|}{\boldsymbol{y}}\right) \sqrt{1 + \left(u'_{y_1}\right)^2}\sqrt{1 + \left(u'_{z_1}\right)^2},$$

where $\boldsymbol{y},\boldsymbol{z} \in \gamma$.

Further, we found the solution of the inverse problem for the function which described relief changes from the middle-level. It was received by using a single-scattering approximation [6, 7]. A nonlinear differential equation is obtained for the numerical solution of which the following scheme was constructed:

$$u_i' = \frac{1}{y_{1,i}}\left(u_{i-1} - l + \sqrt[4]{1 + v_{0,i-1}^2}\ \sqrt{\frac{I(t_i)c^2 t_i^3\left|v_{0,i-1}(l - u_{i-1}) - y_{1,i}\right|}{8\sigma_d J_0 \exp(-\mu c t_i)}}\right), \tag{7}$$

where $t_i = 2c^{-1}\left(y_{1,i}^2 + (l - u_{i-1})^2\right)^{1/2}$.

In the numerical algorithm, the function v_{0_i} is represented as: $v_{0_i} = u'_{i-1}$. For constructing a numerical algorithm, we set two initial conditions: $u(0) = u_0$, $u^{'}(0) = v_0$. The modified Euler's method is used for computational experiments.

In the case of a narrow directivity pattern of the receiving antenna, the problem of remote sensing of the side-scan sonar, moving with a constant velocity $\boldsymbol{V}$ along the axis $\boldsymbol{r_3}$, is reduced to solving the problem (1) - (4) and is solved independently at each probing interval.

The sounding parameters for the computational experiments are presented in Table 1. [8,9]. The purpose of the experiment is to determine the effect of double scattering on the restoration of the seabed relief.

Table 1

Probing parameters [1].

μ, м$^{-1}$	σ_d	c, м/с	J_0	l, м	y_1, м	y_3, м
0.018	1	1500	1	20	[0, 300]	[0, 80]

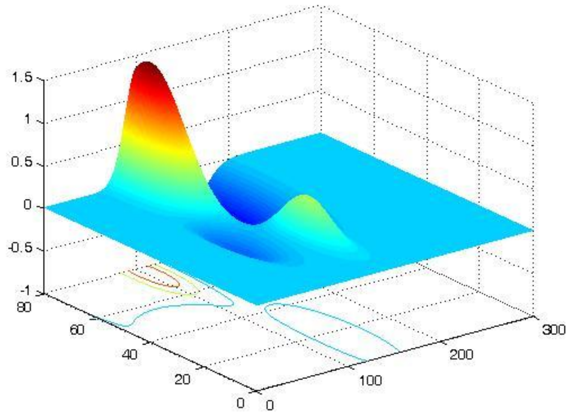

Fig. 1. The exact solution u.

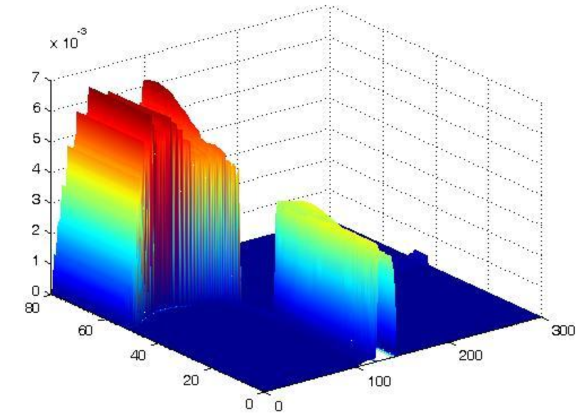

Fig. 2. The double scattering effect on recovery I_2/I.

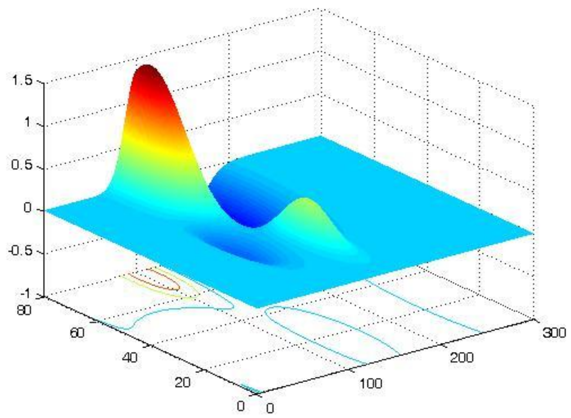

Fig. 3. The retrieval function u in single scattering approximation.

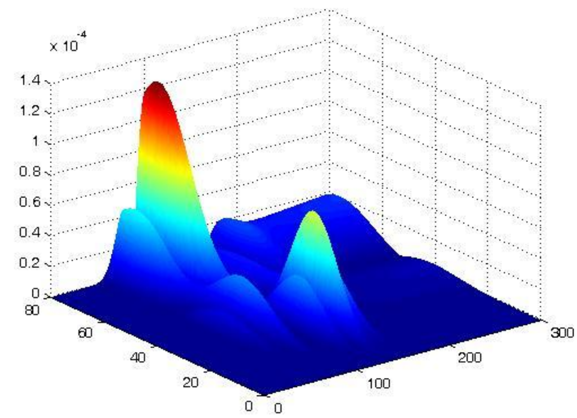

Fig. 4. Error Δu for the single scattering approximation.

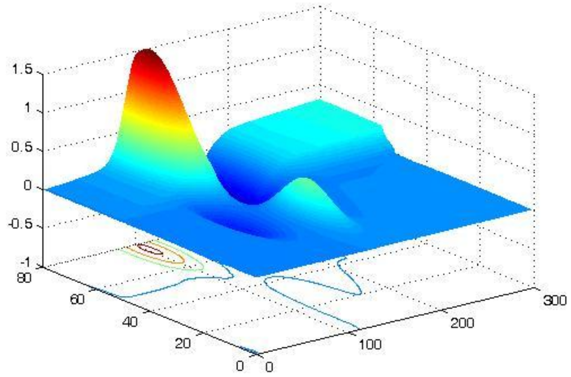

Fig. 5. The retrieval function u in double scattering approximation.

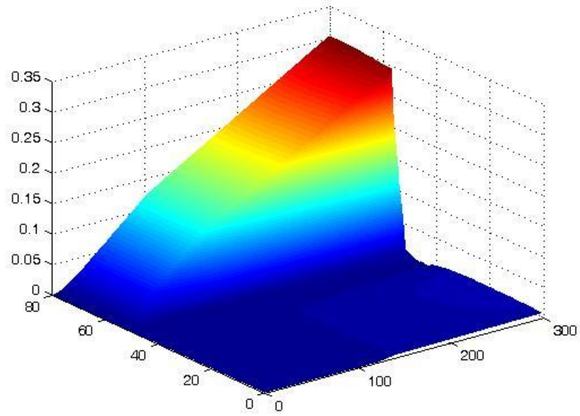

Fig. 6. Error Δu for the double scattering approximation.

Figure 1 presents a graph of the exact solution of the function u, based on which the received signal $I(t)$ was calculated using formula (6).

Figures 3, 4 present a graph of the recovered function u and the error Δu, respectively. As a received signal for plotting 3, the values of signal using only single scattered signal I_1 were taken, i.e. only the first term in the formula (6). As a numerical method for solving the differential equation (7), an iterative predictor-corrector method was chosen with an accuracy of 1.0E-15. Numerical scheme (7) contains the linearization of the derivative on the right-hand side $v_{0_i} = u_{i-1}^{'}$), as can be seen from Figure 4, the maximum error reaches 0.01%, which indicates high accuracy of the numerical method.

Figures 5, 6 show the graph of the recovered function u and the error Δu in the case, when the measured signal $I(t)$ was calculated by formula (6) with allowance for double scattering. To calculate the integral in formula (6), an algorithm was developed for determining the propagation paths of the signal corresponding to double reflection from the bottom.

Figure 2 shows a graph of the ratio of signals I_2 / I, showing the contribution of the double-scattered signal to the total measured signal, which does not exceed 0.1%. Despite such a small contribution, the double-scattered signal significantly affects the recovery of the bottom surface u. The recovery error Δu increases with the sensing range and reaches 0.3 m.

Thus, the solution of the bathymetry problem regarding the double scattered signal was investigated. In the proposed experiments, the double-scattered signal did not exceed 0.1% in the total measured SSS signal, but when solving the bathymetry problem, the recovery error reached 20%. It is worth noting that this result was obtained with a 100% reflection of the signal from the seabed. In the case of partial reflection (~ 10%), the error decreases by a factor of 10 and is ~ 2%.

References

[1] Ageev A. L., Igumnov G. A., Kostousov V. B., Agafonov I. B., Zolotorev V. V., Madison E. A. Aperture synthesizing for multichannel side-scan sonar with compensation of trajectory instability // Izvestiya SFedU. Engineering Sciences. 2013. N 140(3). P. 140—148.

[2] Griffiths G. Technology and Applications of Autonomous // Underwater Vehicles CRC Press. 2002 .

[3] Matvienko Y. V., Voronin V. A., Tarasov S. P., Sknarya A. V., Tutyrin E. V. Some Ways to Improve Technologies for Sonar Survey of the Seabed Using the Autonomous Underwater Unmanned Vehicle // Podvodnye Issledovaniya i Robototekhnika. 2009. N 8(2). P. 4-15.

[4] Prokhorov I. V., Sushchenko A. A. Studying the Problem of Acoustic Sounding of the Seabed Using Methods of Radiative Transfer Theory // Acoustical Physics. 2015 . N 61(3). P. 368-375.

[5] Prokhorov I. V., Sushchenko A. A., Kan V. A., Lyu E. R. Determination of the bottom surface profile // Proceedings of SPIE - The International Society for Optical Engineering. 2017. N 10466 (1046622).

[6] Quijano J. E., Zurk L.M. Radiative transfer theory applied to ocean bottom modeling // The Journal of the Acoustical Society of America. 2009. N 126(4). P. 711-1723.

[7] Prokhorov I. V., Sushchenko A. A. Imaging Based on Signal from Side-Scan Sonar // Applied Mechanics and Materials. 2015. N 756. P. 678-683.

[8] Mendus V. I., Postnov G. A. On Angular Intensity Distribution of High-Frequency Ambient Dynamic Noise of the Ocean // Acoustical Physics. 1993. N 39(6). P. 1107-1116.

[9] Prokhorov I. V., Sushchenko A. A. Analysis of the impact of volume scatteringand radiation pattern on the side-scan sonar images // Proceedings of Meetingson Acoustics. 2015. N 24. P. 005007.